

Spatial dynamics of tree stands disturbance under the Siberian Silk Moth (*Dendrolimus sibiricus*) impact in Central Siberia in 2016–2020 on the base of remote sensing data [†]

Evgenii I. Ponomarev ^{1,2,*}, Andrey A. Goroshko ¹, Evgenii G. Shvetsov ², Nikita D. Yakimov ², Pavel D. Tretyakov ^{1,2}, Svetlana M. Sultson ¹, Pavel V. Mikhaylov ¹

¹ Reshetnev Siberian State University of Science and Technology, 31, Krasnoyarskii Rabochii prospekt, Krasnoyarsk, 660037, Russia, sultson2011@yandex.ru (S.M.S.); ptretyakov99@mail.ru (P.D.T), utrom3@gmail.com (A.A.G.); mihaylov.p.v@mail.ru (P.V.M.)

² Federal Research Center “Krasnoyarsk Science Center, Siberian Branch, Russian Academy of Sciences”, 50/45, Akademgorodok, Krasnoyarsk, 660036, Russia, evg@ksc.krasn.ru (E.I.P), eugeneshvetsov11@yandex.ru (E.G.S), nyakimov96@mail.ru (N.D.Y)

* Correspondence: evg@ksc.krasn.ru; Tel.: +7-3912494092

[†] Presented at the 3rd International Electronic Conference on Forests (IECF2022).

Citation: Ponomarev, E.I.; Goroshko, A.A.; Shvetsov, E.G.; Yakimov, N.D.; Tretyakov P.D.; Sultson, S.M.; Mikhaylov P.V. Spatial dynamics of tree stands disturbance under the Siberian Silk Moth (*Dendrolimus sibiricus* Tschetverikov) impact in Central Siberia in 2016–2020 on the base of remote sensing data. *Environ. Sci. Proc.* **2022**, *4*, x. <https://doi.org/10.3390/xxxxx>

Academic Editor: Firstname Last-name

Published: date

Publisher’s Note: MDPI stays neutral with regard to jurisdictional claims in published maps and institutional affiliations.



Copyright: © 2022 by the authors. Submitted for possible open access publication under the terms and conditions of the Creative Commons Attribution (CC BY) license (<https://creativecommons.org/licenses/by/4.0/>).

Abstract: In this study we have analyzed the spatial dynamics of the forests disturbed by Siberian Silk Moth (*Dendrolimus sibiricus* Tschetverikov (*Lepidoptera: Lasiocampidae*)) in Central Siberia and obtained model equations that fit this dynamics. We considered three sites that experienced silk moth outbreaks in 1993–1996, 2015–2018 and 2018–2020 and used satellite data (NOAA/AVHRR, Terra/MODIS, Landsat/ETM/OLI), field data, digital elevation model, and maps of predominant forests. Silk moth-disturbed areas were classified using NDVI that was calculated for each 15-day period during growing season (April–September). Time series of disturbed forest areas were obtained for three sites located in Krasnoyarsk region (Central Siberia, Russia). Total damaged areas for these sites were 41, 430 and 470 thousand hectares. We obtained formalized descriptions for the temporal dynamics of disturbed area.

Keywords: Siberian Silk Moth; Eastern Siberia; remote sensing; spatial dynamics model

1. Introduction

An analysis of the development of pest outbreak in the forests for each specific case requires the knowledge of the entire complex of parameters that determine the location, growth rate and dynamics of the affected area. It is known from the literature that populations of forest insects can be well described by parametric models that predict the population size under various environmental conditions [1]. At the same time, any numerical predictions based on parametric theoretical models must be validated on the basis of field data, which makes it possible to determine the list of model inputs, parameters and constants [2–5]. The number of field measurements, is usually limited and not always sufficient to calibrate the models that describe the dynamics of the process. When studying insect-disturbed areas it is also important to study the issues of outbreaks locations relative to the physiographic, forest and meteorological conditions (humidity deficit, precipitation regimes, winter and summer temperature regimes, etc.) of the region. This also requires consideration of each individual case [5–12].

In this issue, the studies of the dynamics of disturbed areas that usually have long-term scars on satellite images are of particular interest. It was shown [13, 14] that after the impact of disturbance factors on forest stands, in particular, after the Siberian silk moth

outbreak, changes in the spectral characteristics of damaged areas occur [15–17]. This determines the prospects for using remote sensing data, both for analyzing the forest mortality caused by the complex effects of forest fires, pest outbreaks, etc. [18–21] and to monitor the dynamics of the spatial distribution of pests. Satellite data also make it possible to perform long-term monitoring of the state of damaged forest stands, allowing to classify the disturbance degree [22]. Such approach is now commonly used and widespread in geospatial research in various regions [5,11,23, 24].

The spatio-temporal model of the silk moth outbreak development allows estimating the growth rate of the total area and the main tactical elements of the disturbed area. The results of such studies are the basis for further analysis of the parameters that determine the predominant directions of outbreak propagation under conditions of local relief, aspect and forest growing conditions.

We investigated the following issues: (a) the rate of pest outbreak development in dark coniferous forests of Siberia, (b) modeling the rate of disturbed area increase.

The obtained solutions will make it possible to have a predictive model for the formation and development of the disturbed forest zone, which is necessary at the stage of planning appropriate preventive measures and developing a general strategy for minimizing the consequences under the conditions of repeated outbreaks of Siberian silk moth in the studied areas.

2. Material and Methods

The studies were performed for two sites of dark coniferous taiga in Krasnoyarsk Region, Siberia, Russia: 1) 58°30′–60° N, 88°30′–92° E in the Yenisei region (EnP) with a total area of 4.2 million ha; and 2) 54°45′– 55°05′ N, 95°20′– 99°10′ E in the Irbei district (IrP) with a total area of 904 thousand ha, where Siberian Silk Moth (*Dendrolimus sibiricus* Tschetverikov (*Lepidoptera: Lasiocampidae*)) outbreaks were observed between 2016 and 2020. Figure 1 shows forest areas disturbed by the silk moth according to the moderate spatial resolution data for EnP and IrP.

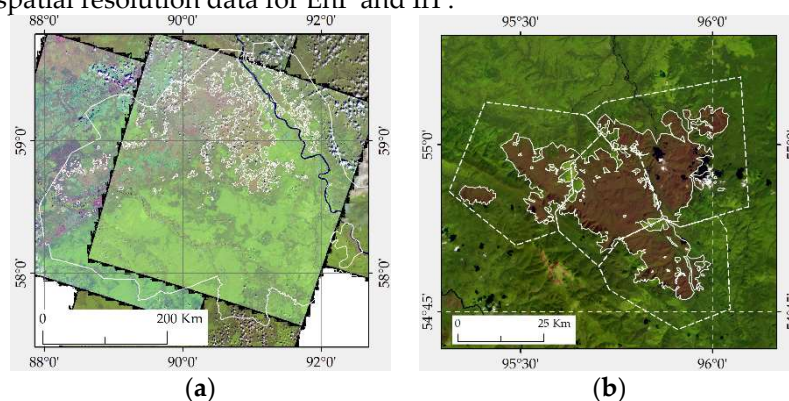


Figure 1. Overview of forests disturbed by silk moth, in (a) EnP for 2020; (b) in IrP for 2020.

The initial data on the areas of disturbed forest zones detected by their spectral features were obtained from Landsat, Sentinel-2 data of moderate spatial resolution (15–30 m) with a frequency of 1–3 months and from Terra/Aqua MODIS data of low spatial resolution (250 m, 1000 m) with a frequency of 14–28 days (MOD13Q1/ MYD13Q1). Thus, the temporal resolution of satellite data for the region of interest was at least once a month in case of moderate resolution data and 2 times a month for the data of low spatial resolution. Time series of disturbed forest areas were obtained for two sites located in Krasnoyarsk region (Central Siberia, Russia).

Vegetation cover map was obtained using “Vega-service” (Database of the Institute of Space Research of the Russian Academy of Sciences, IKI RAS, Moscow, <http://pro-vega.ru/maps/>, accessed 21 September 2022) [25].

3. Results and Discussions

Using the previously described approaches the dynamics of area disturbed by silk moth in the EnP and IrP plots was calculated. The duration of the outbreak in the EnP was 4 years, while for the IrP it was 3 years. The final disturbed areas were 428.6 and 41.5 thousand ha, respectively (Fig. 2).

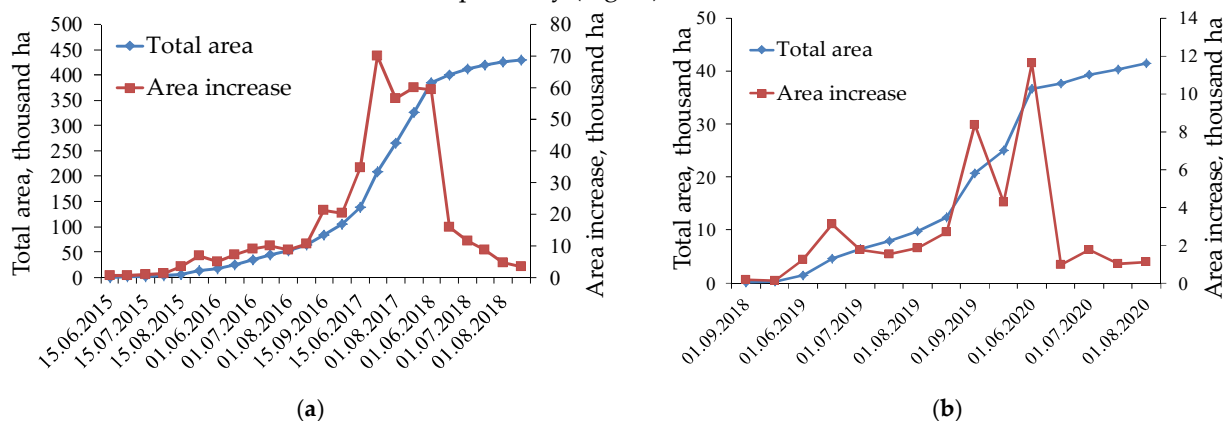


Figure 2. The dynamics of area disturbed by silk moth in EnP (a) and in IrP (b)

The temporal dynamics of the total disturbed area (Fig. 2) can be approximated using the function of normal distribution as follows

$$f(x) = \frac{1}{\sigma\sqrt{2\pi}} e^{-\frac{(x-\bar{x})^2}{2\sigma^2}}, \quad (3.1)$$

where \bar{x} – expected value, σ – standard deviation.

Analyzing the general patterns of development of silk moth disturbed area two phases can be distinguished, that reflect the rate of geospatial spread of the disturbed:

a) a phase of increasing rate of disturbed area growth, which is limited by some characteristic time T_{phase} , unique for each case, that is determined by the change of the pattern of the disturbed area growth, and also

b) the phase of the decreasing rate of area growth and further “saturation” (the maximum value of the disturbed area for the given case).

In case of the IrP, the value of T_{phase} for the time series was 11 months, the initial area of the disturbed forest was 109.4 ha, and the approximating maximum of the area (asymptote) was 35000 ha (Fig. 2).

The type of distribution allows extrapolation of the disturbed area $S = S(t)$ for each phase as an independent function. The general type of the model can be formulated as:

$$S(t) = \begin{cases} S^{\text{ph1}} = A \exp(Bt + C) + D, & \text{for } t < T_{\text{phase}} \\ S^{\text{ph2}} = E \ln(Ft + G) + H, & \text{for } t \geq T_{\text{phase}} \end{cases} \quad (3.2)$$

and the corresponding set of coefficients (K_i), which determine the amplitude of the initial phase of the disturbed zone development (A), the rate of area growth (B, F), the state of the disturbed zone at the time of the beginning of logarithmic growth (E) and additive terms (C, D, G, H). Here, the phase of the increasing rate of the area growth (exponential increase) is designated S^{ph1} , and the phase of the decreasing rate of the area growth and further saturation is S^{ph2} .

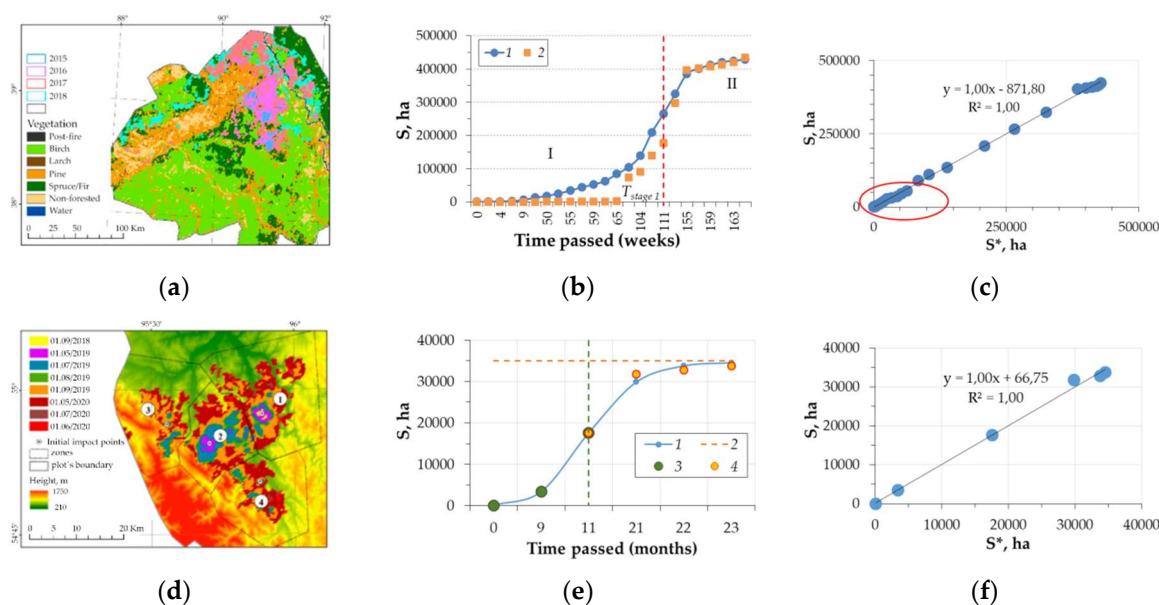


Figure 3. The dynamics of the area disturbed by silk moth for EnP в 2015–2018 гг. (a) and IrP в 2018–2020 гг. (d), ASTER GDEM [26] is shown as background; Model of the monthly distribution of the area disturbed by silk moth for EnP which approximates the Terra/MODIS data with 14 days temporal resolution, where I corresponds to exponential growth (phase "I"), II is the approximating of the final stage. For IrP (b), where 1 is the experimental data, 2 – approximating the maximum of the final area, 3 – model solution for the phase of exponential area growth, 4 – model solution for the phase of decreasing rate of area growth (logarithmic approximation) and further saturation (e); Plot of correlation field for experimental measurement data (based on satellite data) and model calculation results for EnP (c) and for IrP (f)

Table 1. Coefficients of the equations for the model of disturbed zone growth

IrP, 2018–2020				
Model	Model Coefficients (2)			
Phase I: $Aexp(Bx+C)+D$	<i>A</i>	<i>B</i>	<i>C</i>	<i>D</i>
	0.91	0.82	0.86	1.00
Phase II: $E \ln(Fx+G)+H$	<i>E</i>	<i>F</i>	<i>G</i>	<i>H</i>
	22497.42	0.187	0.07	558.35
EnP, 2015–2018, $T_{\text{phase}} = 111$ weeks				
Model	Model Coefficients (3.2)			
Phase I: $Aexp(Bx+C)+D$	<i>A</i>	<i>B</i>	<i>C</i>	<i>D</i>
	0.989	0.100	0.986	1.00
Phase II: $E \ln(Fx+G)+H$	<i>E</i>	<i>F</i>	<i>G</i>	<i>H</i>
	60.903	0.007	7.704	0.101

The solution (Fig. 3a) obtained based on the model approximations (2), (3), agrees well with the experimental data set and has a high level of correlation ($r \sim 0.99$) (Table 1).

A silk moth outbreak in the Yenisei region in 2015–2018 was characterized by the spatial scale of the disturbed area that have limited the use of satellite data of moderate spatial resolution (Landsat, Sentinel-2). Thus, the Terra/MODIS data were unique data source on the dynamics of the silk moth outbreak development.

In the first approximation the solution for the dynamics of the disturbed area contains a significant discrepancy for the stage of exponential growth (Fig. 3 "I") with the

114
115
116
117
118
119
120
121
122

123

124
125
126
127
128
129
130
131
132

$T_{\text{phase 1}} = 111$ weeks, since the area of the disturbed area on the initial stages of 2015 and 2016 was significantly lower than the final values delineated using satellite data in 2017–2018.

With all the assumptions of the first approximation of the model, the obtained solution (Table 1) for the disturbed area dynamics is in good agreement with the experimental data set and has a high level of correlation ($r \sim 0.97$), which is shown in the correlation field plot (Fig. 3c, f).

The restrictions imposed on the spatial advancement of the disturbed area are associated with natural boundaries (such as non-forested areas, ridges, valley complexes, rivers, etc.), heterogeneity of vegetation and forest composition, the time of the outbreak origination, as well as spatial and temporal peculiarities of the origination of secondary (multiple) locations of pest outbreaks, anisotropy of physical and geographical characteristics, microrelief and local conditions. Determination of the directions of the predominant advancement of the disturbed area requires a comprehensive analysis of all factors listed above [5,10–12,23,24]. In addition, these indicators can be input conditions that regulate the rate of spread of the disturbed area and individual tactical elements, as well as the degree of damage to forest stands [22].

4. Conclusions

The results obtained represent the formalized descriptions of the temporal distribution of the disturbed area consistent with data series based on satellite data for silk moth outbreaks in the EnP (in 2015–2018) and IrP (in 2018–2020) regions of the Krasnoyarsk region, Siberia, Russia.

We obtained formalized descriptions for the temporal dynamics of disturbed area. Coefficients for the model solution were optimized using the Lagrange multiplier method and non-linear generalized downgrading gradient method. It is shown that the systems of empirical solutions adequately ($R^2 \sim 0.97$) fit field data and can be used to simulate silk moth outbreaks under similar conditions. We have tested model regression equations for predicting the azimuthal spread of damaged area with a confidence level of $r = 0.60–0.68$.

It was shown that it is necessary to additionally identify and analyze inter-seasonal periods of disturbed area dynamics to improve the accuracy of the model. Individual seasons should be considered as independent sub-periods, which must be accompanied by refined coefficients of model equations when forming a general solution. A set of obtained solutions reflects the probable range of silk moth outbreak scenarios.

Author Contributions: Conceptualization, E.P.; methodology, E.P., N.Y., E.S.; software, E.P., N.Y., E.S., A.G.; validation, E.P., N.Y., S.S., P.M. and A.G.; formal analysis, E.P., E.S., A.G.; investigation, E.P., N.Y., and P.T.; resources, E.P., S.S., P.M.; data curation, E.P., S.S.; writing—original draft preparation, E.P., N.Y., and E.S.; writing—review and editing, E.P., E.S.; visualization, N.Y., A.G., P.T.; supervision, E.P.; project administration, S.S.; funding acquisition, S.S., P.M. All authors have read and agreed to the published version of the manuscript."

Funding: This study was supported by the Ministry of Education and Science of the Russian Federation (theme «Fundamental principles of forest protection from entomo- and phyto- pests in Siberia» No. FEFE-2020-0014) and the subject of project no. 0287-2021-0040 (KSC SB RAS).

Institutional Review Board Statement: Not applicable

Informed Consent Statement: Not applicable.

Data Availability Statement: Publicly available datasets were analyzed in this study. These data can be found here: <http://pro-vega.ru/maps/> (accessed on 27 August 2022) and <https://worldview.earthdata.nasa.gov/> (accessed on 27 August 2022).

Acknowledgments: The satellite data-receiving equipment used was provided by the Center of Collective Usage of Federal Research Center "Krasnoyarsk Science Center, Siberian Branch of Russian Academy of Sciences", Krasnoyarsk, Russia.

Conflicts of Interest: The authors declare no conflict of interest.

References

1. Kovalev, A.V.; Ovchinnikova, T.M. Development of simulation models for dynamics of forest pest numbers. *Contemp. Probl. Ecol.* **2010**, *2*, 27–35. 185
2. Morris, R.F. The development of predictive equations for the spruce budworm based on keyfactor analysis. *The Dynamics of Epidemic Spruce Budworm Populations. Memoirs of Entomological Society of Canada* **1963**, *95(31)*, 116–129. 186
DOI:10.4039/ENTM9531116-1. 187
3. Mawby, W.D.; Hain, P.P.; Doggett, C.A. Endemic and epidemic populations of southern pine beetle: Implications of the two-phase model for forest managers. *Forest Sci.* **1989**, *35*, 1075–1087. 188
4. Iskhakov, T.R.; Sukhovol'skii, V.G.; Ovchinnikova, T.M.; Tarasova, O.V. A population and energy model of a forest insect outbreak. *Biophysics*, **2007**, *52(4)*, 440–444. DOI:10.1134/S0006350907040161. 189
5. Möykkynen, T.; Pukkala, T. Modelling of the spread of a potential invasive pest, the Siberian moth (*Dendrolimus sibiricus*) in Europe. *For. Ecosyst.* **2014**, *1*, 10. DOI:10.1186/s40663-014-0010-7. 190
6. Mikhailov, Ju.Z.; Sumina, N.Yu. Siberian moth *Dendrolimus superans* (Butler, 1877) and control of it in Irkutsk region. *Bajk. zool. J.* **2012**, *3(11)*, 25–29. (In Russian) 191
7. Leontiev, D.F. Distribution and forecasting of the population of the Siberian silkmoth (scientific review). *Intern. Journal. Applied and fundamental research* **2015**, *11*, 705–709. (in Russian) 192
8. Pavlov, I.N.; Litovka, Y.A.; Golubev, D.V.; Astapenko, S.A.; Chromogin, P.V. New outbreak of *Dendrolimus sibiricus* tschetv. in Siberia (2012–2017): monitoring, modeling and biological control. *Contemp. Probl. Ecol.* **2018**, *11(4)*, 406–419. 193
DOI:10.1134/S1995425518040054. 194
9. Lyamtsev, N.I. Assessment and forecast of Siberian moth mass propagation risks in the Krasnoyarsk krai forests. *Izvestia Sankt-Peterburgskoj lesotekhnicheskoy akademii* **2019**, *228*, 294–311. DOI: 10.21266/2079-4304.2019.228.294–344 (in Russian) 195
10. Sultson, S.M.; Goroshko, A.A.; Verkhovets, S.V.; Mikhaylov, P.V.; Ivanov, V.A.; Demidko, D.A.; Kulakov, S.S. Orographic Factors as a Predictor of the Spread of the Siberian Silk Moth Outbreak in the Mountainous Southern Taiga Forests of Siberia. *Land* **2021**, *10(2)*, 1–16. DOI:10.3390/land10020115. 196
11. Sultson, S.M.; Goroshko, A.A.; Mikhaylov, P.V.; Demidko, D.A.; Ponomarev, E.; Verkhovets, S.V. Improving the Monitoring System Towards Early Detection and Prediction of the Siberian Moth Outbreaks in Eastern Siberia. *Proceedings* **2021**, *68*, 5. 197
DOI:10.3390/IECE-10403. 198
12. Kovalev, A.; Soukhovolsky, V. Analysis of Forest Stand Resistance to Insect Attack According to Remote Sensing Data. *Forests* **2021**, *12(9)*:1188. DOI:10.3390/f12091188. 199
13. Fedotova, E.V.; Im, S.T.; Kharuk, V.I. Analysis of the spatial confinement of areas of taiga forests disturbed by the Siberian silk moth according to small-scale remote sensing data. *Interexpo GEO-Siberia* **2007**, *2(2)*, 206–210. (In Russian) 200
14. Im, S.T.; Fedotova, E.V.; Kharuk, V.I. Spectrodiametric satellite imagery in the analysis of the outbreak zone of mass reproduction of the Siberian silk moth. *Journal of Siberian Federal University. Engineering & Technologies* **2008**, *1(4)*, 346–358. (In Russian) 201
15. Wolfe, R.E.; Roy, D.P.; Vermote, E. MODIS Land Data Storage, Gridding, and Compositing Methodology: Level 2 Grid. *IEEE Transactions on Geoscience and Remote Sensing* **1998**, *36(4)*, 1324–1338. DOI:10.1109/36.701082. 202
16. Didan, K.; Munoz, A.B.; Solano, R.; Huete, A. MODIS Vegetation Index User's Guide Version 3.00, June 2015 (Collection 6). 203
17. Knyazeva, S.V.; Koroleva, N.V.; Eidlina, S.P.; Sochilova, E.N. Health of vegetation in the area of mass outbreaks of Siberian moth based on satellite data. *Contemp. Probl. Ecol.* **2019**, *12(7)*, 743–752. DOI:10.1134/S1995425519070114. 204
18. Kharuk, V. I.; Ranson, K.J.; Im, S.T. Siberian silkmoth outbreak pattern analysis based on SPOT VEGETATION data. *Int. J. Remote Sens.* **2009**, *30(9)*, 2377–2388. DOI:10.1080/01431160802549419. 205
19. Bartalev, S.; Egorov, V.; Zharko, V.; Loupian, E.; Plotnikov, D.; Khvostikov, S.; Shabanov, N. Land cover mapping over Russia using Earth observation data. Moscow, Russian Academy of Sciences' Space Research Institute, Russia, 2016; pp. 208. (In Russian) 206
20. Kharuk, V.I.; Antamoshkina, O.A. Impact of Silkmoth Outbreak on Taiga Wildfires. *Contemp. Probl. Ecol.* **2017**, *10(5)*, 556–562. 207
DOI:10.1134/S1995425517050055. 208
21. Bartalev, S.A.; Stytsenko, F.V. An assessment of the forest stands destruction by fires based on the remote sensing data on a seasonal distribution of burnt areas. *Contemp. Probl. Ecol.* **2021**, *2*, c. 115–122. DOI:10.31857/S0024114821020029. 209
22. Vaganov, E.A.; Shashkin, A.V.; Kharuk, V.I.; Khlebopros, R.G.; Sukhovolsky, V.G.; Gaevsky, N.A.; Degermendzhi, A.G.; Gubanov, V.G. *Ecological biophysics. Vol. 2. Biophysics of land and water ecosystems*. Eds. Gitelzon, I.I.; Pechurkin, N.S. Moscow, Logos, Russia, 2002. 360 p. ISBN 5-94010-073-2. (In Russian) 210
23. Kharuk, V.I.; Demidko, D.A.; Fedotova, E.V.; Dvinskaya, M.L.; Budnik, U.A. Spatial and temporal dynamics of Siberian silk moth large-scale outbreak in dark-needle coniferous tree stands in Altai. *Contemp. Probl. Ecol.* **2016**, *9(6)*, 711–720. 211
DOI:10.1134/S199542551606007X. 212
24. Kharuk, V.I.; Im, S.T.; Soldatov, V.V. Siberian silkmoth outbreaks surpassed geoclimatic barrier in Siberian Mountains. *Journal of Mountain Science* **2020**, *17*, 1891–1900. DOI:10.1007/s11629-020-5989-3. 213
25. Loupian, E.A.; Bourtsev, M.A.; Proshin, A.A.; Kashnitskiy, A.V.; Balashov, I.V.; Bartalev, S.A.; Konstantinova, A.M.; Kobets, D.A.; Radchenko, M.V.; Tolpin, V.A.; Uvarov, I.A. Usage Experience and Capabilities of the VEGA-Science System. *Remote Sensing* **2022**, *14(1)*, 77. DOI:10.3390/rs14010077. 214
26. Abrams, M.; Crippen, R.; Fujisada, H. ASTER Global Digital Elevation Model (GDEM) and ASTER Global Water Body Dataset (ASTWBD). *Remote Sens.* **2020**, *12(7)*, 1156. DOI:10.3390/rs12071156. 215

184

185

186

187

188

189

190

191

192

193

194

195

196

197

198

199

200

201

202

203

204

205

206

207

208

209

210

211

212

213

214

215

216

217

218

219

220

221

222

223

224

225

226

227

228

229

230

231

232

233

234

235

236

237

238

239

240

241

242